Edge Contrast Failure Analysis on Vision Angle of Human Eyes for Curve Displays

Bor-Jiunn Wen and T. S. Liu

***Abstract*—For curve displays, the purpose of this study is to present edge contrast failure analysis (ECFA) method on the vision angle of human eyes. In order to analyze edge contrast of curve display images, a flexible cholesteric liquid crystal display is bent for different radii of curvature by using a flexible-characteristic inspection system. To simulate the human eye factors, a charge-coupled device colorimeter is utilized based on ECFA to analyze a maximum vision angle of human eyes with respect to curve displays under different radii of curvature. According to analysis results, a designer or maker of curve displays can design large-vision-angle and comfortable curve-display products for human being.**

***Index Terms*—Curve display, edge contrast failure analysis (ECFA), flexible cholesteric liquid crystal display, flexible-characteristic inspection system, vision angle of human eyes.**

I. Introduction

With rapid advance in semiconductor technology as well as in panel display industry, designs for all kinds of electronic consumer products, including cellular phones, notebook computers, monitor display, and other digital household appliances are becoming more and more diversified. Nowadays, flat panel displays can not satisfy people who demand for comfortable lifestyle. In response to customer requests, a 360° cylindrical display or a curve display with better viewing angle enables the audience to watch a high quality image from a large range of viewing angles. Compared with flat panel displays, according to [1] with a viewing angle within $\pm 15^{\circ}$, a curve display can avoid head movement. For advertising usage, 360° cylindrical displays maximize the precious space of people sight, so as to achieve the best possible advertising effectiveness. Unfortunately, when a person stands at a fixed place and watches a curve display, he can not see a clear whole view of images on the curve display. The reason is that some parts of the reflective or emissive lights from pictures and characters on the curve display can not go into human eyes according to the law of reflection [2]. For image assessment, the contrast-sensitivity function (CSF) is usually utilized for a measure of fundamental spatio–chromatic properties of the human visual system [3], [4]. For example, a high image contrast at higher spatial frequencies demonstrates the observer's ability to see lines and edges in detail. As a result, when an image has a low edge contrast, a clear view of the image is not easy to be recognized by human eyes. Because few lights from pictures and characters at some vision angles go into human eyes, the edge contrasts are too low to exhibit a clear whole view on the curve display, where the vision angle of human eyes is double of the angle between the normal of the curve display and the center position of the image. The vision angle of human eyes depends on radii of curvature of curve displays and the distance between human eyes and curve display. Accordingly, it is desired to design radii of curvature of curve displays to maintain edge contrasts of pictures and characters for a large vision angle of human eyes. Although the inspection of flat-panel-display contrast is a mature technique [5], there is no literature dealing with edge contrast analysis for curve displays. In addition, many studies have found visual factors that differentiate dyslexic from normal readers, including sensitivity to contrast [6]–[8]. To analyze vision contrast, letter identification is used frequently in practical assessment [9], [10], including the measurement of visual acuity at high contrast [11] and low contrast [12], as well as the measurement of contrast sensitivity using large [13] and small [14] letter sizes. Scoring procedures have been proposed that are based on the number of individual letters that are identified correctly [15], [16]. However, a complicated letter-image identification process is required for vision contrast analysis by using instruments whether all letters are equally identifiable in these measurements [17], [18]. Therefore, this study creates a novel edge contrast failure analysis (ECFA) method on vision angle of human eyes with respect to curve displays. In order to analyze edge contrast of curve display images, a flexible cholesteric liquid crystal display (Ch-LCD) is bent for different radii of curvature by using a flexible-characteristic inspection system (FCIS) [19]. Different widths of line patterns are presented on a 6″ flexible Ch-LCD. To simulate the human eye factors, a charge-coupled device (CCD) colorimeter is utilized based on ECFA to analyze the edge contrast of different widths of line patterns on curve displays under different radii of curvature for a maximum vision angle of human eyes. The theory, simulation and experimental results of ECFA for the vision angle of human eyes are presented in this study. According to analysis results, a designer or maker of curve displays can design large-vision-angle and comfortable curve-display products.

Manuscript received December 10, 2011; revised February 29, 2012; accepted March 02, 2012. Date of publication April 25, 2012; date of current version June 28, 2012.

B.-J. Wen is with the Department of Mechanical Engineering, National Chiao Tung University, Hsinchu 30010, Taiwan, and also with the Center for Measurement Standards, Industrial Technology Research Institute, Hsinchu 30011, Taiwan.

T. S. Liu is with the Department of Mechanical Engineering, National Chiao Tung University, Hsinchu 30010, Taiwan (e-mail:tsliu@mail.nctu.edu.tw).

Color versions of one or more of the figures are available online at http://ieeexplore.ieee.org.

Digital Object Identifier 10.1109/JDT.2012.2190495

II. Theory of Edge Contrast Failure Analysis

Consider a vision model of human eyes based on a curve display with line-pattern images as shown in Fig. 1.

In this model, the focal plane of a human eye is on the X-axis plane with a vision angle. Assume that line patterns on the curve display are projected on the focal plane in the vision model of

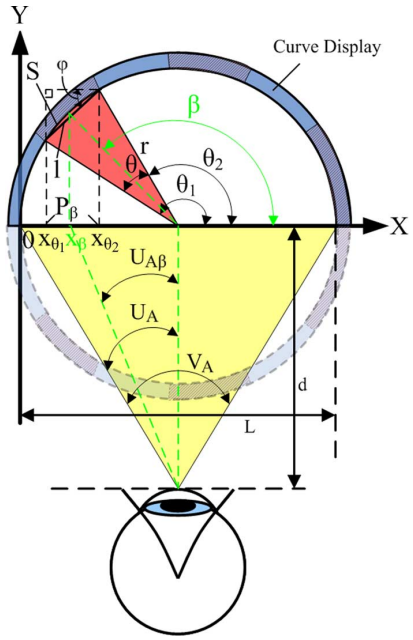

Fig. 1. Vision model of human eyes with respect to curve display with line-pattern images.

human eyes. A vision angle $\mathrm{V}_{\mathrm{A}\beta}$ of a human eye at β angle is double of the angle between the normal of the curve display and the image center projected on X-axis where $\mathrm{U}_{\mathrm{A}\beta} = \frac{1}{2}\mathrm{V}_{\mathrm{A}\beta}$ is a human viewing angle. In practice, the concave and convex models have the same optical-geometry inference. In this study, a vision model of human eyes based on a concave curve display is analyzed by using ECFA. In Fig. 1, slash areas are line patterns under r radius of curvature of the curve display and the width of each line pattern is S. The width of the line pattern at β angle projected on the X-axis is denoted as P_β. Accordingly,

$$\begin{cases} \theta = \theta_1 - \theta_2 \\ \mathrm{S} = \theta \mathrm{r} = \mathrm{r}(\theta_1 - \theta_2) \\ \varphi = \theta_2 - \frac{\pi - \theta}{2} \\ 1 = 2\mathrm{r}\sin\frac{\theta}{2} \\ \beta = \frac{\theta_1 + \theta_2}{2} \\ \mathrm{P}_\beta = \mathrm{x}_{\theta_2} - \mathrm{x}_{\theta_1} \end{cases} \tag{1}$$

where $\theta_1 > \theta_2 > \theta$. Since

$$\mathrm{x}_{\theta_2} - \mathrm{x}_{\theta_1} = 1\cos\varphi = 2\mathrm{r}\sin\frac{\theta}{2}\cos\left(\theta_2 - \frac{\pi - \theta}{2}\right) \tag{2}$$

Equation (2) is rewritten as

$$\mathrm{x}_\alpha = 2\mathrm{r}\sin\frac{\pi - \alpha}{2}\cos\left(\alpha - \frac{\alpha}{2}\right) = 2\mathrm{r}\cos^2\frac{\alpha}{2} \tag{3}$$

where $\theta_1 = \pi$ and $\theta_2 = \alpha$. Therefore, by assuming that $\mathrm{x}_{\theta_1} = 2\mathrm{r}\cos^2(\theta_1/2)$ and $\mathrm{x}_{\theta_2} = 2\mathrm{r}\cos^2(\theta_2/2)$, (1) leads to

$$\begin{aligned} \mathrm{P}_\beta &= \mathrm{x}_{\theta_2} - \mathrm{x}_{\theta_1} = 2\mathrm{r}\left(\frac{1+\cos\theta_2}{2} - \frac{1+\cos\theta_1}{2}\right) \\ &= 2\mathrm{r}\sin\frac{\theta_1+\theta_2}{2}\sin\frac{\theta_1-\theta_2}{2} \\ &= 2\mathrm{r}\sin\beta\sin\frac{\mathrm{S}}{2\mathrm{r}}. \end{aligned} \tag{4}$$

Since $\mathrm{x}_\beta = 2\mathrm{r}\cos^2(\beta/2) = \mathrm{r}(1+\cos\beta)$ where x_β is the center position of the line pattern projected on the X-axis, one has

$$\sin\beta = \sqrt{1 - \left(\frac{\mathrm{x}_\beta}{\mathrm{r}} - 1\right)^2}. \tag{5}$$

Substituting (5) into (4) gives

$$\mathrm{P}_\beta(\mathrm{x}_\beta) = 2\mathrm{r}\sin\frac{\mathrm{S}}{2\mathrm{r}}\sqrt{1 - \left(\frac{\mathrm{x}_\beta}{\mathrm{r}} - 1\right)^2}. \tag{6}$$

Accordingly, P_β depends on x_β with given S and r. When an edge contrast of the line pattern decreases to one level, P_β becomes small and does not maintain the original width. Here the original width is the width of each line pattern S. The level is called edge contrast failure analysis limitation (ECFAL). In other words, when a decreasing P_β is smaller than ECFAL, it is easy for human eyes to judge the difference between decreasing P_β and S. According to [20], visual acuity of human eyes (VAHE) is a measure of the spatial resolution of the visual processing system for human eyes. For example, when the size of an image is smaller than VAHE, it can not be recognized by human eyes. Therefore, in ECFA, the difference between the S and ECFAL represents VAHE depending on the distance between the focal plane of a human eye and human eyes. It implies that when P_β is between S and ECFAL, P_β is still recognized as S.

Accordingly, ECFAL is defined in this study as

$$\mathrm{ECFAL} = S - \mathrm{VAHE} \tag{7}$$

where VAHE is a visual acuity of human eyes. Substituting (7) into (6) gives

$$\begin{aligned} \mathrm{P}_{\mathrm{ECFAL}}(\mathrm{x}_{\mathrm{ECFAL}}) &= \mathrm{ECFAL} \\ &= \mathrm{S} - \mathrm{VAHE} \\ &= 2\mathrm{r}\sin\frac{\mathrm{S}}{2\mathrm{r}}\sqrt{1 - \left(\frac{\mathrm{x}_{\mathrm{ECFAL}}}{\mathrm{r}} - 1\right)^2} \end{aligned} \tag{8}$$

Solving (8) gives

$$\mathrm{x}_{\mathrm{ECFAL}} = \mathrm{r}\left(1 \pm \sqrt{1 - \left(\frac{\mathrm{S} - \mathrm{VAHE}}{2\mathrm{r}\sin\frac{\mathrm{S}}{2\mathrm{r}}}\right)^2}\right). \tag{9}$$

As a result, the difference between line patterns is not easy to judge for human eyes within the range between two $\mathrm{x}_{\mathrm{ECFAL}}$ solutions. The maximum vision angle of human eyes is obtained as

$$\mathrm{V}_\mathrm{A} = \frac{360}{\pi}\tan^{-1}\left(\frac{\mathrm{r}\sqrt{1 - \left(\frac{S - \mathrm{VAHE}}{2\mathrm{r}\sin\frac{\mathrm{S}}{2\mathrm{r}}}\right)^2}}{\mathrm{d}}\right) \tag{10}$$

where d is the distance between human eyes and the projecting plane. To avoid head movement, it requires a viewing angle within $\pm 15^\circ$ for curve displays [1]. Therefore, in the vision model of human eyes

$$2d\tan(15^\circ) = L \geq W \tag{11}$$

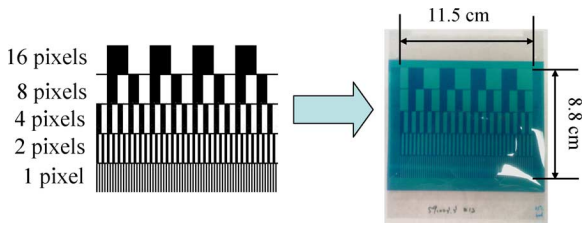

Fig. 2. Line patterns on 30-dpi-resolution flexible Ch-LCD.

where d is the width of the focus plane of human eyes and W is the width of the curve display. In other words, the limitation of ECFA is

$$d \geq \frac{W}{2\tan(15^\circ)} = 1.87\ \mathrm{W} \tag{12}$$

Using (10), a designer or maker of curve displays can design optimal S, r, and d magnitudes of curve-display products for a large vision angle of human eyes by using ECFA.

III. Measurement Apparatus

In order to analyze a maximum vision angle of human eyes with respect to curve displays under different radii of curvature by using ECFA, a two-color 30-dpi-resolution flexible Ch-LCD is utilized. According to [21], any stimulus to the visual system can be described by visual size, luminance contrast, color difference, retinal image quality, and retinal illumination. Because flexible Ch-LCDs are reflective displays, a good measurement geometry to overcome noises of retinal image quality and illumination for measuring optical properties is important [5]. Therefore, this study designs 1, 2, 4, 8 and 16-pixel widths of line patterns to present on a 6″ 30-dpi-resolution flexible Ch-LCD for different visual sizes, as shown in Fig. 2.

According to [22] and [5], two large-diffuse D65 light sources are utilized to provide a 500 lux with 95% uniform illumination on a 10 cm^2 flat square in 500 mm front of a CCD colorimeter (AMA 400 KC), as shown in Fig. 3.

To simulate the human eye factors, in Fig. 3, two light sources are placed at $\pm 45^\circ$ incidence angles. In addition, a flexible Ch-LCD is fixed at 500 mm along a normal direction of the curve display by using a six-axis motion stage with a feedback signal of a laser rangefinder. The maximum horizontal viewing angle with a 6″ flexible Ch-LCD in 500 mm front of the colorimeter is $\pm 6.6^\circ$ in this measurement apparatus. Therefore, according to (12)

$$d = 500 \geq 1.87W = 1.87 \times 115 = 215.05 \tag{13}$$

satisfies the limitation of ECFA. Because the depth of focus of the colorimeter is 200 mm and the focal plane is at the peak or trough of the Ch-LCD, this study can catch all images of the Ch-LCD under different radii of curvature. Moreover, there are several sources of error associated with array detectors in practice [5]. To reduce image error, the colorimeter is calibrated in compliance with [5] for a flat-field correction by using a 5-cm-radius exit port of an integrating sphere with 99% uniform luminance in this study. In addition, an FCIS [19] is used to control radii of curvature of flexible Ch-LCDs.

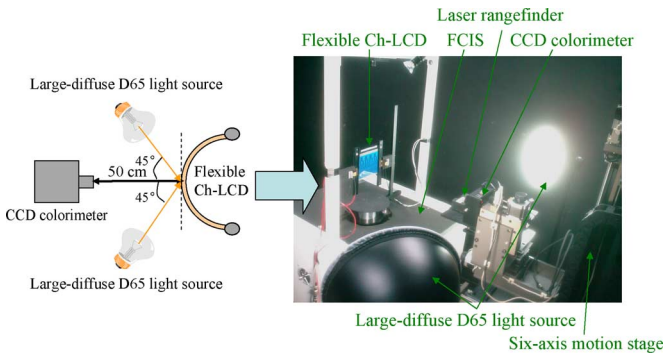

Fig. 3. Measurement geography apparatus for ECFA.

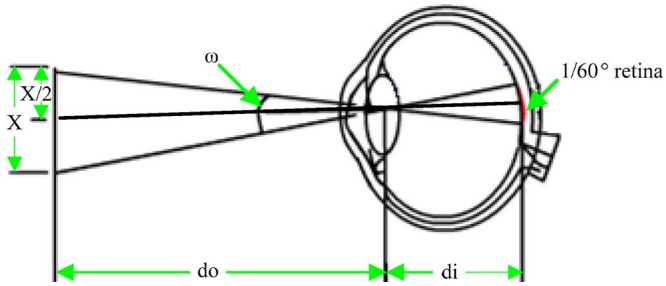

Fig. 4. Visual acuity model of human eyes.

IV. Simulation and Experimental Results

This section deals with a vision model of human eyes described by Section II. In order to validate the novel ECFA method for human vision angle, this study investigates simulation and experimental results of a vision measurement apparatus of human eyes based on the ECFA method described in Section III. According to [23], the standard definition of normal visual acuity of human eyes is the ability to resolve a spatial pattern separated by a visual angle of one minute of arc. Since one degree contains 60 minutes, a visual angle of one minute of arc is 1/60th of a degree. Therefore, assume a visual acuity model of human eyes as shown in Fig. 4.

According to Section III and [23], both and d in (10) equal to 500 mm and ω is 1/60° in Fig. 4. As a result, $\mathrm{X} = 0.145$ mm is prescribed as VAHE in this study. In simulations and experiments, 1-pixel-width line patterns are utilized for high resolution measurements of human vision angles. Therefore, S in (10) is 0.85 mm. Suppose that a concave bending for a Ch-LCD display is a positive curve-radius condition, whereas a convex bending is a negative curve-radius condition. Therefore, based on theoretical derivation of ECFA in Section II with $S = 0.85$ mm and $\mathrm{VAHE} = 0.145$ mm, (10) concerning the maximum vision angle of human eyes is utilized for simulating a vision model of human eyes with different radii of curvature. Accordingly, the numerical simulation of the maximum vision angle of human eyes is carried out by using a MATLAB software.

In experiments, a colorimeter is utilized with a measurement apparatus described in Section III. Firstly, a 6″ 30-dpi-resolution Ch-LCD with line patterns is bent for one radius of curvature by FCIS. Secondly, a colorimeter captures an image of the Ch-LCD and then grabs one-dimension line image, as shown in

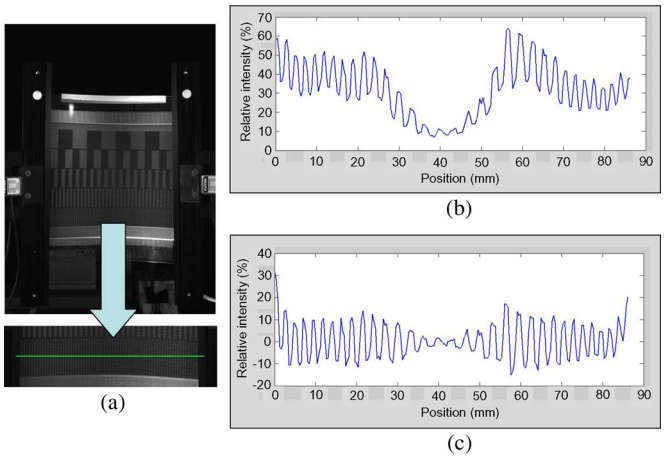

Fig. 5. (a) One-dimension line image grab of flexible Ch-LCD under 80 mm radius of curvature; one-dimension line image signals: (b) before and (c) after employing the Fourier transform, Gaussian filter, and inverse Fourier transform.

Fig. 5(a). In Fig. 5, the Ch-LCD is bent for 80 mm radius of curvature. Thirdly, according to the law of reflection [2], because nonuniform illumination induces low frequency noise and low edge contrasts under different radii of curvature on the center position of the Ch-LCD, this study applies the Fourier transform and Gaussian filter defined by [24] for the line image to reduce image noise and enhance line image signals on the center position of the Ch-LCD. Fig. 5(b) and (c) shows one-dimension line image signals before and after employing the Fourier transform, Gaussian filter, and inverse Fourier transform, respectively. In Fig. 5(b) and (c), a full-width at half-maximum is a width of the line pattern.

Fourthly, the positions of line patterns are obtained by solving the solutions when the relative intensity of the line pattern is zero. The difference between a solution and the next solution is the width of the line pattern. Fifthly, transform the positions of line patterns into human viewing angles and let a human vision angle be zero at maximum $\mathrm{P}_{\beta}(\mathrm{U}_{\mathrm{A}\beta})$. Sixthly, in Fig. 1, when x_{β} is less and less than or greater and greater than r, $|\mathrm{U}_{\mathrm{A}\beta}|$ becomes larger and larger than U_{Ar}. In other words, according to (6), when $|\mathrm{U}_{\mathrm{A}\beta}|$ is larger and larger than U_{Ar}, $\mathrm{P}_{\beta}(\mathrm{x}_{\beta})$ becomes smaller than $\mathrm{P}_{\beta}(\mathrm{r})$. Accordingly, (6) and $\mathrm{P}_{\beta}(\mathrm{U}_{\mathrm{A}\beta})$ are parabola equations and also second-order polynomial equations. As a result, a fitting curve of human viewing angles versus widths of line patterns is obtained by applying a second-order polynomial fitting. Finally, a vision angle threshold of human eyes is calculated by using ECFAL. As a result, a maximum vision angle of human eyes is obtained when the width of line patterns is ECFAL. Fig. 6 shows the procedure of measuring the vision angle of human eyes for flexible Ch-LCDs by using ECFA.

Fig. 7 depicts the measurement result of human viewing angle for a flexible Ch-LCD at 80 mm radius of curvature by using ECFA. In Fig. 7, the black dots represent measurement data of line patterns, the blue solid line is line-pattern fitting curve, and the red broken line is ECFAL. Simulation and experimental results of measuring a maximum vision angle of human eyes under different radii of curvature by using ECFA are shown in Fig. 8. The blue solid line represents a simulation result, and the red dots are the experimental results. Because the maximum horizontal viewing angle in this measurement apparatus

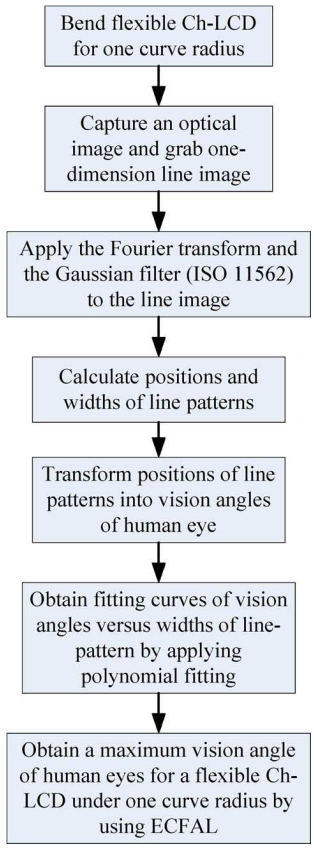

Fig. 6. Procedure of measuring the vision angle of human eyes for flexible Ch-LCDs by using ECFA.

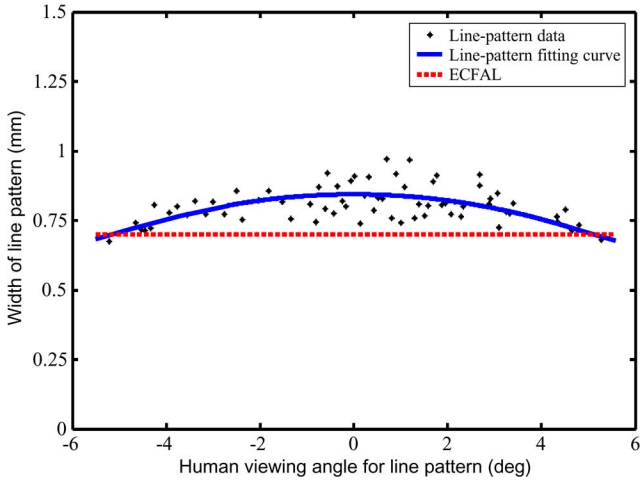

Fig. 7. Measurement result of human viewing angle for a flexible Ch-LCD at 80 mm radius of curvature by using ECFA.

described in Section III is $\pm 6.6^{\circ}$ and a flexible Ch-LCD is not bent to smaller than 10 mm radius of curvature by using FCIS, simulation results are presented from -105 mm to -10 mm radii of curvature and from 10 to 105 mm radii of curvature.

According to simulation and experimental results, the following conclusions are drawn.

1) Simulation and experimental results validate the proposed ECFA method on vision angles of human eyes based on the measurement apparatus described in Section III.

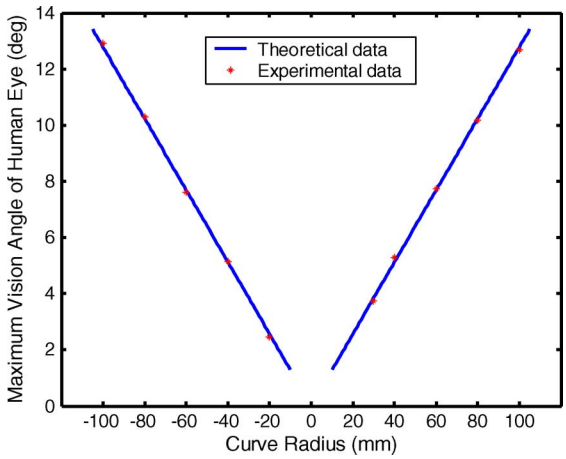

Fig. 8. Simulation and experimental results of maximum vision angle of human eyes.

TABLE I
SIMULATION AND EXPERIMENTAL RESULTS OF MAXIMUM VISION ANGLE OF HUMAN EYES CORRESPONDING TO RADII OF CURVATURE

Radius of curvature (mm)	Simulation result of vision angle of human eyes (deg)	Experimental result of vision angle of human eyes (deg)	Difference (deg) (simulation - experimental result)
-100	12.773	12.925	-0.152
-80	10.233	10.277	-0.044
-60	7.684	7.603	0.081
-40	5.127	5.136	-0.009
-20	2.565	2.471	0.094
30	3.846	3.731	0.115
40	5.127	5.278	-0.151
60	7.684	7.738	-0.054
80	10.233	10.165	0.068
100	12.773	12.685	0.088

2) In Fig. 7, there are some larger measurement errors near the center of the Ch-LCD under concave 80 mm radius of curvature. The reason is that nonuniform illumination under concave conditions is easy to induce low edge contrasts and image noise on the center image of the flexible Ch-LCD. According to Figs. 5(b) and (c), although the Fourier transform, Gaussian filter, and inverse Fourier transform can reduce image noise and enhance line image signals on the center position of the Ch-LCD, other image noise is also enhanced by enhancing line image signals. Therefore, low edge contrasts and image noise on the center image of the Ch-LCD result in larger measurement errors.
3) Table I depicts simulation and experimental results in measuring a maximum vision angle of human eyes by using ECFA. In Table I, differences between simulation and experimental results are larger than the others when a flexible Ch-LCD is under smaller concave radius of curvature. The reason is the same as Conclusion 2.
4) Although after image processing there is still some noise on measurement results due to nonuniform illumination under different radii of curvature and measurement disturbance signals, experimental results are consistent with simulation results. Accordingly, this study has presented an effective measurement method dealing with the vision angle of human eyes with respect to curve displays.
5) To catch the whole images of concave or convex curve displays, the depth of focus of the CCD requires greater than width sizes of curve displays.
6) According to the simulation and experimental results, ECFA is a useful analysis method concerning vision angle of human eyes for curve displays.

V. CONCLUSION

This study has presented a new analysis method ECFA dealing with vision angles of human eyes for curve displays according to simulation and experimental results. In addition, this study also has presented an effective measurement method for vision angles of human eyes. Accordingly, a designer or maker of curve displays can design large-vision-angle and friendly curve-display products for human being by using this measurement method and ECFA.

ACKNOWLEDGMENT

The authors thank Display Technology Center of Industrial Technology Research Institute for providing flexible cholesteric liquid crystal displays.

REFERENCES

[1] *Ergonomic Requirements for Office Work With Visual Display Terminals (VDTs): Ergonomic Requirements and Measurement Techniques for Electronic Visual Displays*, ISO 9241-300 subseries, International Organization for Standardization, 2008.
[2] E. Hecht, *Optics*, 4th ed. Reading, MA: Addison Wesley, 2002.
[3] S. Westland, H. Owens, V. Cheung, and I. Paterson-Stephens, "Model of luminance contrast-sensitivity function for application to image assessment," *Color Res. Appl.*, vol. 31, pp. 315–319, 2006.
[4] E. Peli, "Contrast sensitivity function and image discrimination," *J. Opt. Soc. Amer. A*, vol. 18, pp. 283–293, 2001.
[5] *Flat Panel Display Measurements Standard* , Version 2.0, FPDM Task Group, Video Electronics Standards Assoc. (VESA), 2001.
[6] B. A. O'Brien, J. S. Mansfield, and G. E. Legge, "The effect of contrast on reading speed in dyslexia," *Vision Res.*, vol. 40, pp. 1921–1935, 2000.
[7] B. C. Skottun, "The magnocellular deficit theory of dyslexia: The evidence from contrast sensitivity," *Vision Res.*, vol. 40, pp. 111–127, 2000.
[8] M. J. Williams, G. W. Stuart, A. Castles, and K. I. McAnally, "Contrast sensitivity in subgroups of developmental dyslexia," *Vision Res.*, vol. 43, pp. 467–477, 2003.
[9] K. R. Alexander, X. Wei, and D. J. Derlacki, "The effect of contrast polarity on letter identification," *Vision Res.*, vol. 33, pp. 2491–2497, 1993.
[10] D. G. Pelli, C. W. Burns, B. Farell, and D. C. Moore-Page, "Feature detection and letter identification," *Vision Res.*, vol. 46, pp. 4646–4674, 2006.
[11] F. L. Ferris, III, V. Freidlin, A. Kassoff, S. B. Green, and R. C. Milton, "Relative letter and position difficulty on visual acuity charts from the early treatment diabetic retinopathy study," *Amer. J. Ophthalmol.*, vol. 116, pp. 735–740, 1993.
[12] D. Regan and D. Neima, "Low-contrast letter charts as a test of visual function," *Ophthalmol.*, vol. 90, pp. 1192–1200, 1983.
[13] D. G. Pelli, J. G. Robson, and A. J. Wilkins, "The design of a new letter chart for measuring contrast sensitivity," *Clinical Vision Sciences*, vol. 2, pp. 187–199, 1988.

[14] J. Rabin, "Luminance effects on visual acuity and small letter contrast sensitivity," *Optometry and Vision Sci.*, vol. 71, pp. 685–688, 1994.
[15] I. L. Bailey, M. A. Bullimore, T. W. Raasch, and H. R. Taylor, "Clinical grading and the effects of scaling," *Invest. Ophthalmol. Visual Sci.*, vol. 32, pp. 422–432, 1991.
[16] D. B. Elliott, M. A. Bullimore, and I. L. Bailey, "Improving the reliability of the Pelli–Robson contrast sensitivity chart," *Clinical Vision Sciences*, vol. 6, pp. 471–475, 1991.
[17] H. Bouma, "Visual recognition of isolated lower-case letters," *Vision Res.*, vol. 11, pp. 459–474, 1971.
[18] G. E. Legge, D. G. Pelli, G. S. Rubin, and M. M. Schleske, "Psychophysics of reading—I. Normal vision," *Vision Res.*, vol. 25, pp. 239–252, 1985.
[19] B. J. Wen and T. S. Liu, "Flexible-characteristics inspection system for flexible substrates by using image feedback control," *Displays*, vol. 32, pp. 296–307, 2011.
[20] C. Ware, *Information Visualization: Perception for Design*. Waltham, MA: Morgan Kaufmann, 2000.
[21] R. P. Boyce, *Human Factors in Lighting*, 2nd ed. Abingdon, U.K.: Taylor & Francis, 2003.
[22] S. Kubota, "Reflectance and contrast measurements of reflective liquid crystal displays," *Displays*, vol. 18, pp. 79–83, 1997.
[23] B. Yost, Y. Haciahmetoglu, and C. North, "Beyond visual acuity: The perceptual scalability of information visualizations for large displays," in *In Proc. CHI 2007*. New York: ACM Press, 2007, pp. 101–110.
[24] *Geometrical Product Specifications (GPS)-Surface Texture: Profile Method—Metrological Characteristics of Phase Correct Filters*, ISO 11562, , 1996.

Bor-Jiunn Wen received the B.S. degree from Tankang University, Taipei, Taiwan, in 2001, the M.S. degree from National Chaio Tung University, Hsinchu, Taiwan, in 2003, both in mechanical engineering, and currently working toward the Ph.D. degree in mechanical engineering from National Chaio Tung University, Hsinchu, Taiwan.

His research interests include mechanics, control-system design, opto-mechatronics, optical and color measurements, automatic optical inspection, and flexible-display characteristic measurement.

T. S. Liu received the B.S. degree from National Taiwan University in 1979, and the M.S. and Ph.D. degrees from the University of Iowa in 1982 and 1986, respectively, all in mechanical engineering.

Since 1987, he has been with the Department of Mechanical Engineering, National Chiao Tung University, Taiwan, where he is currently a professor. In 1991, he was a visiting researcher with the Institute of Precision Engineering, Tokyo Institute of Technology. In 1998, he was also a visiting researcher with the Institute of Precision Engineering, Swiss Federal Institute of Technology, Zurich, Switzerland. His research interests are in opto-mechatronics, dynamics aand control of mechatronic systems, and flexible-display characteristic measurement.